International Scientific Conference 20 UNITECH 26

INTERNATIONAL SCIENTIFIC CONFERENCE
19-21 November 2026
GABROVO

EFFECT OF COOLING RATE AND POTENTIAL CHOICE ON THE SOLIDIFICATION KINETICS AND PHASE STABILITY OF PURE LITHIUM

Murat Celtek[1], Cem Canan[2], Unal Domekeli[3]

[1]Faculty of Education, Trakya University, 22030, Edirne – Türkiye
[2]Edirne Vocational College of Technical Science, Trakya University, 22030, Edirne – Türkiye
[2]Dept. of Physics, Trakya University, 22030, Edirne – Türkiye

……
**Corresponding author: mceltek@trakya.edu.tr and muratceltek@gmail.com*

Abstract

In this study, the heating and cooling processes of pure lithium (Li) were investigated using molecular dynamics (MD) simulations with EAM and TB potentials. The structural evolution of the system during these processes has been discussed in detail using pair distribution functions (g(r)), static structure factors (S(q)), lattice parameters, and Honeycutt-Andersen bonded-pair analysis methods. There was good agreement between the results obtained from the EAM potential and the experimental data from the literature, including the melting point, lattice parameter, heat capacity, and the g(r) and S(q) curves. At a slow cooling rate of 0.5 K/ps, the EAM confirmed the dissolution of the liquid icosahedral structure and its transformation into a stable bcc phase exceeding 90%. Conversely, the strong bonding character of the TB potential suppressed the bcc structure, leading to an artificial hcp+fcc accumulation. Meanwhile, the high cooling rate of 20 K/ps inhibited crystallization, thereby stabilizing the amorphous structure. In summary, the study clearly shows that many-body potentials and kinetic parameters are critical for accurately predicting phase transformations and glass formation mechanisms at the atomic scale in Li-based materials.

Keywords: pure lithium, molecular dynamics, EAM/TB potentials, pair distribution function, solidification kinetics, phase stability.

INTRODUCTION

Lithium (Li) is an important material, particularly in high-energy-density lithium-metal batteries, thanks to its low atomic mass and high electrochemical activity. However, the atomic and structural behavior of pure Li is more complex than expected for a simple alkali metal. Recent studies have shown that the energy differences between the various crystal phases of Li are small and that harmonic effects significantly impact phase stability [1]. The close energy balance among the bcc, fcc, and 9R structures requires a detailed account of temperature and atomic motion to accurately model Li's structural behavior [1]. The atomistic modeling of pure Li's liquid and solid phases continues to be an important research topic. Vella et al. [2] compared the properties of Li, including its melting curve, liquid density, and liquid structure, by using different EAM potentials. They demonstrated that the choice of potential significantly impacts the obtained results. In a more recent study, Srinivasan et al. [3] developed a machine-learning model based on atomic cluster expansion (ACE) to describe solid and liquid Li. They demonstrated that the density, viscosity, diffusion coefficient, and melting temperature of liquid Li could be modeled in

This is an open access article licensed under Creative Commons Attribution 4.0 International
Print ISSN: 1313-230X, Online ISSN: 3033-1404

agreement with experimental and ab initio results. These studies demonstrate that the interaction potential employed in atomistic simulations of pure Li is a critical factor in the reliability of the results [2, 3]. In terms of the solidification process, the cooling rate is one of the fundamental kinetic parameters that determines how long it takes for atoms to reorganize from a liquid structure into an ordered solid structure [4, 5]. Indeed, molecular dynamics (MD) studies of various metallic systems have shown that changes in cooling rate directly affect solidification temperature, nucleation mechanisms, and final atomic structure. Therefore, examining the structural evolution of the system cooled at different rates is crucial to determining the final crystal structure of pure lithium and understanding how local atomic order develops during solidification. Thus, our study uses molecular dynamics (MD) simulations to focus on the structural behavior of pure Li under different cooling rates. To emphasize the significance of selecting an interatomic potential for this process, we used two different potentials (EAM [6] and Tight-Binding (TB) [7] potentials) and compared their effects. In summary, this study aims to thoroughly evaluate the solidification kinetics of pure Li at the atomic level and compare the predictive capabilities of different potential models for this process.

EXPOSITION

In the EAM approach, the total energy of the system includes the embedding energy, which depends on the local electron density at each atom's location, in addition to the pair interaction term between atoms, and is generally expressed as follows [6]:

$$E_T = \frac{1}{2}\sum_{i,j,i\neq j}^{N}\varphi_{ij}(r_{ij}) + \sum_{i}^{N}F_i(\rho_i), \qquad (1)$$

where $\varphi_{ij}(r_{ij})$ represents the pair interaction term, and $F_i(\rho_i)$ represents the embedding energy, which depends on the local electron density. On the other hand, the TB approach defines metallic bonding through electronic interactions between atomic orbitals, thereby allowing changes in the local atomic environment to be directly reflected in the energy. These two approaches have distinct physical foundations that enable an assessment of the potential dependence of Li's thermal and structural behavior. In this context, the total energy of the TB potential is expressed as follows in the second-moment approximation [7, 8]:

$$E_T = -\left\{\sum_{j\neq i}\xi^2 \exp\left[-2q\left(\frac{r_{ij}}{r_0}-1\right)\right]\right\}^{1/2} + \sum_{j\neq i}A\exp\left[-p\left(\frac{r_{ij}}{r_0}-1\right)\right] \qquad (2)$$

For more detailed information on the mathematical framework, parameterization details, and applications of the EAM and TB potentials, see the relevant references [9–12].

In this study, pure Li systems were modeled using the DL_POLY MD simulation package [13]. The initial structure was generated as a bcc crystal, and the equations of motion were integrated using the Leapfrog algorithm with a time step of 1 fs. Heating and cooling processes were performed under the NPT ensemble. Temperature was controlled using the Berendsen thermostat, and pressure was controlled using the Berendsen barostat. In general, temperature increments of 50 K were used while heating the system from 0 K to 1000 K. However, 10 K steps were adopted near the melting point to increase thermal resolution. On the other hand, the cooling process was carried out in the opposite direction, from 1000 K down to 0 K in 50 K increments. To determine the effect of cooling rate on solidification behavior, three cooling rates were applied: 5, 0.5, and 0.05 K/ps. The effects of cooling rate and potential selection on the solidification process of Li were evaluated by comparing the temperature-energy, temperature-volume, and atomic structural properties obtained using both potentials.

This study used the EAM potential parameterized by Al-Awad et al. [14]. Although it was originally developed for liquid Li, we tested its applicability to the solid bcc phase at low temperatures before conducting our simulations. For comparison, we evaluated the TB parameterization proposed by Karolewski [15], which was fitted to the cohesive energy, lattice parameter, elastic constants, and vacancy formation energy of bcc Li. As shown in Table 1, the EAM method produces highly consistent results with experimental data in the low-temperature and room-temperature solid regimes ($T \leq 300$ K).

Table 1. *Comparison of physical properties calculated from the present study using EAM and TB potentials for pure Li with experimental and other literature results.*

	This work		
	EAM	**TB**	**Exp.**
$E_{coh.}$ (eV/atom)	1.67	1.93	1.63[a]
a_0(Å)	3.51	3.30	3.49[a]
	3.53	3.34	3.51[b]
T_m(K)	520	360	454[a]
$\alpha_L(x10^{-6}, K^{-1})$	32.3	60.96	46[c]
$\alpha_V(x10^{-6}, K^{-1})$	96.8	182.9	138[c]
$C_p(Jmol^{-1}K^{-1})$	26.65	30.47	24.86[c]
$\rho(g/cm^3)$	0.534	0.642	0.542[c]
	0.526	0.620	0.534[b]

[a]Ref [16], [b]Ref [17], [c]Ref [18]

The calculated cohesive energy, lattice parameter, atomic density and solid-state heat capacity (C_p= 26.65 $Jmol^{-1}K^{-1}$) show excellent agreement with the following experimental references: 1.63 eV/atom, 3.49–3.51 Å, 0.534–0.542 g/cm³, and 24.86 $Jmol^{-1}K^{-1}$, respectively. Conversely, the TB potential shows a clear tendency to over-binding in the solid phase. This leads to an overestimation of the cohesive energy (1.93 eV/atom) and an artificial contraction of the lattice parameter (3.30–3.34 Å), which consequently overestimates the solid density by nearly 16%.

Overall, the EAM potential accurately reflects the structural and thermodynamic properties of solid bcc Li. However, future studies should examine the elastic constants (C_{11}, C_{12} and C_{44}) more closely to verify its mechanical stability and anisotropic behavior in the solid phase.

To extend this assessment to a wider temperature range, the temperature dependence of the lattice parameter was investigated between 0 and 1000 K (see Fig. 1). As shown in Fig. 1, the lattice parameters obtained via EAM-MD in this study demonstrate reasonable agreement with the experimental data reported by Beg et al. [19] and Owen et al. [20] in the solid phase at 300 K, as well as with the ACE-MD results of Srinivasan et al. [3]. However, compared to experimental and other MD results, TB-MD simulations predict lower lattice parameters across the entire temperature range. This observed difference is consistent with the tendency of the TB potential, as presented in Table 1, to form stronger bonds. This leads to a more compact unit cell and, consequently, a higher solid density.

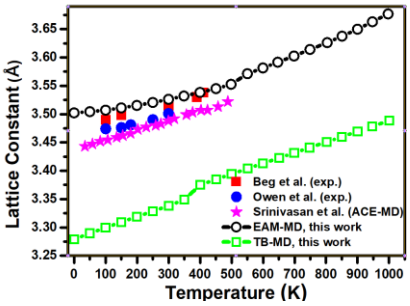


Fig. 1. *Comparison of the temperature dependence of the lattice parameter of bcc Li with experimental results and other findings from the literature.*

As the temperature increases, a pronounced increase in the lattice parameters is observed at around 360 K for the TB-MD method and at around 520 K for the EAM-MD method. This suggests that the two methods predict different melting points for pure bcc Li. Overall, the close agreement with experimental data, particularly at low temperatures, demonstrates that the EAM potential more realistically represents the

lattice parameter and temperature-dependent structural behavior of bcc Li than the TB-MD potential. To enable a detailed comparison of the structural and atomic packing characteristics of the liquid phase, the pair distribution function (g(r)) and the static structure factor (S(q)) were calculated from the EAM-MD and TB-MD simulations at a temperature of 750 K. Detailed information about these structural analysis methods and their associated theoretical calculations can be found in fundamental literature sources [21–23]. Fig. 2(a) and (b) present the g(r) (or S(q)) results obtained from the simulations comparatively with experimental X-ray (or Neutron) diffraction (XRD) (or ND) data at 725 K [24]. Figure 1(a) shows that the EAM-MD model accurately captures electron screening and multi-body interactions in the melt. It does so by matching the first-neighbor distance ($r_1 \approx 3.0$ Å) and peak amplitude with experimental XRD data with high precision. By contrast, the first peak in the TB-MD method has shifted to smaller r-values (r <3.0 Å) and its intensity has decreased. This situation stems from the short-range repulsive potential barrier (repulsive core) in the TB-MD potential being too hard, which predicts a more diffuse atomic arrangement in the first coordination shell. Due to the Fourier transform relationship, these characteristic differences in real space are directly reflected in the S(q) scattering spectrum in reciprocal space.

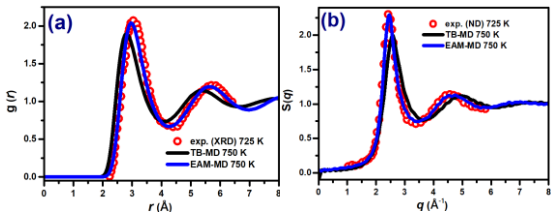


Fig. 2. *Comparison of liquid (a) g(r) and (b) S(q) curves obtained from EAM-MD and TB-MD simulations at 750 K with experimental results at 725 K.*

Examining the S(q) curves in Fig. 2(b) shows that EAM-MD's success at distance r_1 caused the primary scattering peak ($q_1 \approx 2\pi/r_1$) to coincide exactly with the experimental peak position. The leftward shift of g(r) in TB-MD caused the main peak in the S(q) spectrum to shift to the right toward higher q-values and resulted in the peak remaining broader and lower due to underestimation of collective density fluctuations. The phase alignment of the damped oscillations in the high-q region confirms that the EAM potential accurately models liquid-phase ordering without creating artificial constructive or destructive interference.

To examine changes in the microstructure of the system in greater detail, we used the Honeycutt-Andersen (HA) bond-pair analysis method, a powerful topological tool that is widely used in the literature to characterize local structural environments and interpret phase transformations [25, 26].

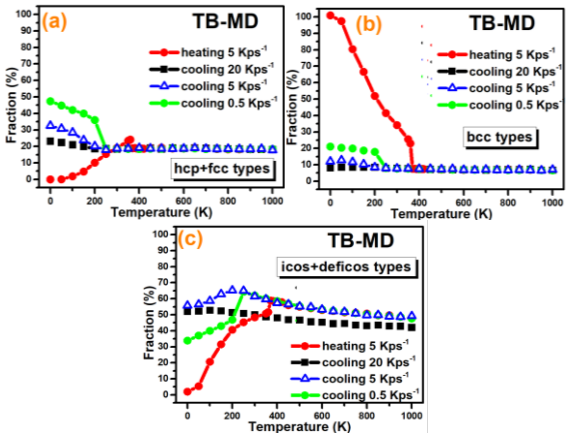


Fig. 3. *Temperature-dependent variation of (a) hcp+fcc, (b) bcc, and (c) icos+deficos HA types obtained at different cooling rates (20, 5, 0.5 K/ps) for the TB-MD potential.*

The results of the analyses clearly demonstrate that the solidification kinetics, local atomic evolution, and phase stability of pure Li are highly sensitive to both the chosen interaction potential and the applied cooling rate. The EAM potential was successful in maintaining its demonstrated results regarding lattice parameters, cohesive energy, and liquid structure factors within the realm of solidification kinetics. Under a slow cooling regime of 0.5 K/ps, the EAM potential realistically simulated the collapse of the liquid-phase-specific icosahedral (icos) and deformed-icosahedral

(deficos) short-range order (1431+1541+1551) and its replacement by the thermodynamically stable bcc (1441+1661) phase with an excess of 90%. In contrast, the TB potential, the nature of its excessive binding, and its hard, repulsive core structure suppressed the bcc phase during solidification. This resulted in the accumulation of close-packed fcc+hcp (1421+1422) structures at unrealistically high levels (around 50%) within the local structure. From a kinetic perspective, reducing the cooling rate allowed the atoms to diffuse, which was necessary for stable bcc nucleation. In contrast, in the system cooled more rapidly (20 K/s), crystallization was suppressed because the atoms lacked the time to rearrange. This indicates that the atoms in the system froze in random positions and the system remained stable in an amorphous/glassy state.

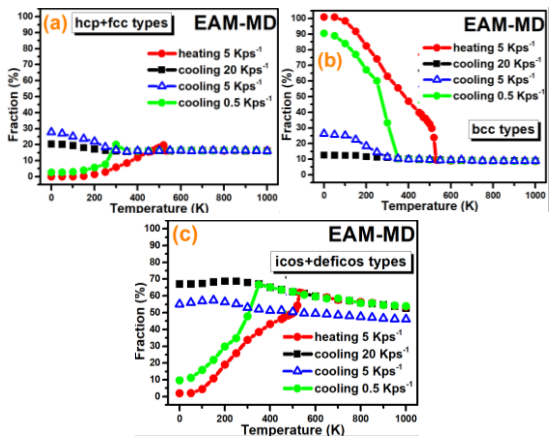


***Fig. 4.**. Temperature-dependent variation of (a) hcp+fcc, (b) bcc, and (c) icos+deficos HA types obtained at different cooling rates (20, 5, 0.5 K/ps) for the EAM-MD potential.*

CONCLUSION

In this study, the structural changes of pure bcc Li during heating and cooling processes have been comprehensively investigated using classical MD simulations with EAM and TB potentials. The effect of cooling rate on the cooling process was investigated using three different cooling rates (20, 5, and 0.5 K/ps). The EAM potential demonstrated good agreement with experimental data regarding the g(r) and S(q) curves calculated for liquid Li, in addition to accurately predicting the low-temperature lattice parameter, cohesive energy, and heat capacity values of bcc Li. Furthermore, HA analyses have definitively shown that the icosahedral order in the liquid phase breaks down at a slow cooling rate (0.5 K/ps) and gives way to a stable bcc phase exceeding 90%. In contrast, it was found that the TB potential suppresses the development of the stable bcc phase during the rapid cooling process due to its strong bonding character and hard repulsive core effects. Instead, it has been observed that hcp+fcc types, positioned close to one another, emerge at high levels during this process. For both potentials, the high cooling rate of 20 K/ps restricted the mobility of the atoms, freezing the melt's icosahedral network structure in the solid phase and trapping the system in an amorphous or glassy state. The current results clearly demonstrate that EAM-based many-body potentials should be preferred to accurately model the phase transformation dynamics, glass transition behavior, and crystallization process of pure Li. Furthermore, they are encouraging for the investigation of the structural, dynamic, and mechanical properties of pure Li under various conditions.

REFERENCE

[1] Shen Y, Xie W. Decoding lithium's subtle phase stability with a machine learning force field. J Mater Chem A 2025; 13: 7119–7124.

[2] Vella JR, Stillinger FH, Panagiotopoulos AZ, et al. A Comparison of the Predictive Capabilities of the Embedded-Atom Method and Modified Embedded-Atom Method Potentials for Lithium. J Phys Chem B 2015; 119: 8960–8968.

[3] Srinivasan P, Puri S, Pacho Dominguez K, et al. Atomic cluster expansion interatomic potentials for lithium: Investigating the solid and liquid phases. Phys Rev B 2025; 112: 054108.

[4] Celtek M, Sengul S. Effects of cooling rate on the atomic structure and glass formation process of Co90Zr10 metallic glass

investigated by molecular dynamics simulations. Turkish J Phys 2019; 43: 11–25.
[5] Celtek M. In-depth investigation of the effect of cooling rate on structural and dynamic properties of Cu54Hf46 alloy by molecular dynamics simulations. J Non Cryst Solids 2025; 664: 123615.
[6] Daw MS, Baskes MI. Embedded-atom method: Derivation and application to impurities, surfaces, and other defects in metals. Phys Rev B 1984; 29: 6443–6453.
[7] Cleri F, Rosato V. Tight-binding potentials. Comput Simul Mater Sci 1991; 205: 233–253.
[8] Senturk Dalgic S, Celtek M. Glass forming ability and crystallization of CuTi intermetallic alloy by molecular dynamics simulation. J Optoelectron Adv Mater 2011; 13: 1563–1569.
[9] Senturk Dalgic S, Celtek M. Liquid -to-glass transition in bulk glass-forming Cu55-xZr45Agx alloys using molecular dynamic simulations. EPJ Web Conf 2011; 15: 03009.
[10] Celtek M. Saf Kalsiyum Elementinin Isıtma Sürecinin Moleküler Dinamik Benzetim Yöntemi ile İncelenmesi. Bitlis Eren Üniversitesi Fen Bilim Derg 2021; 10: 803–815.
[11] Celtek M, Domekeli U. Molecular dynamic simulatıon study of melting Point of L12-Cu3Au alloy. In: Internatıonal Scıentıfic Conference 16-17 November, Gabrovo. Gabrovo-Bulgaria, 2018.
[12] Celtek M, Domekeli U. Investigation of the melting process of niobium using two different potentials: A molecular dynamics simulation study. In: Internationla Scientefic Conference 20-22 November. Bulgaria/Gabrovo, 2025.
[13]Smith W, Forester TR. DL_POLY_2.0: A general-purpose parallel molecular dynamics simulation package. J Mol Graph 1996; 14: 136–141.
[14]Al-Awad AS, Batet L, Sedano L. Parametrization of embedded-atom method potential for liquid lithium and lead-lithium eutectic alloy. J Nucl Mater 2023; 587: 154735.
[15] Karolewski MA. Tight-binding potentials for sputtering simulations with fcc and bcc metals. Radiat Eff Defects Solids 2001; 153: 239–255.
[16] Kittel C. Introduction to the physics of the solid state. University. John Wiley & Sons, Inc, 1986.
[17] John R. Rumble. CRC Handbook of Chemistry and Physics. 102nd ed. London, New York: CRC Press / Taylor & Francis Group, 2021.
[18] Touloukian YS, Kirby RK, Taylor RE, et al. Thermal Expansion Metallic Elements and Alloys, Thermophysical Properties of Matter - The TPRC Data Series. Volume 12. New York: Plenum, 1975.
[19] Beg MM, Nielsen M. Temperature dependence of lattice dynamics of lithium 7. Phys Rev B 1976; 14: 4266–4273.
[20] Owen EA, Williams GI. X-Ray Measurements on Lithium at Low Temperatures. Proc Phys Soc Sect A 1954; 67: 895–900.
[21] Waseda Y. The Structure of Non-Crystalline Materials-Liquids and Amorphous Solids. New York: London: McGraw-Hill, 1981.
[22] Faber TE, Ziman JM. A theory of the electrical properties of liquid metals. Philos Mag 1965; 11: 153–173.
[23] Allen MP, Tildesley DJ. Computer Simulation of Liquids. Oxford University PressOxford. Epub ahead of print 22 June 2017. DOI: 10.1093/oso/9780198803195.001.0001.
[24] Olbrich H, Ruppersberg H, Steeb S. Experimental Determination of the Form and Structure Factor of Molten Lithium. Zeitschrift fur Naturforsch - Sect A J Phys Sci 1983; 38: 1328–1336.
[25] Honeycutt JD, Andersen HC. Molecular dynamics study of melting and freezing of small Lennard-Jones clusters. J Phys Chem 1987; 91: 4950–4963.
[26]Guder V, Celtek M, Celik FA, et al. Crystallization analysis and determination of Avrami exponents during isothermal annealing and the effect of cooling rate on the evolution of the atomic structure of Pd78Si16Cu6 alloy: A molecular dynamics simulation study. J Non Cryst Solids 2023; 602: 122067.